JOURNAL OF COMPUTATIONAL PHYSICS 41, 233–244 (1981)

Implicit Moment Particle Simulation of Plasmas*

RODNEY J. MASON

Los Alamos Scientific Laboratory, University of California, Los Alamos, New Mexico 87545

Received August 5, 1980

It is shown that an implicit E field can be obtained from Poisson's equation with the aid of the lower two fluid moment equations, permitting stable particle simulations for $\omega_p \Delta t \gg 1$ and $\Delta x/\lambda_D \gg 1$, where ω_p and λ_D are the plasma frequency and Debye length, respectively. In the quasi-neutral limit the effect of this E is to provide just the predicted current required to drive all present deviations in the total charge density to zero in the next cycle. In near vacuum, or with $\omega_p \Delta t \gg 1$, the field expression reduces to the standard form used with conventional leap-frog schemes. Sample applications are discussed.

1. INTRODUCTION

For efficient simulations of plasmas there is often a need to calculate the dominant evolving hydrodynamic behavior of electrons using a time step Δt large compared to the plasma period, $\omega_p \Delta t \gg 1$, with the minimum spatial resolution Δx large compared to a Debye length, $\Delta x/\lambda_D \gg 1$.

This has led to the development of hybrid models [1–3] for situations in which the electrons are expected to be isothermal, adiabatic, or nearly Maxwellian. Where more detailed information about the electron distribution has been required, the need for efficiency has encouraged the invention of time-filtering [4], and orbit-averaging [5] techniques.

These techniques have been supplemented by methods originally developed to model the electron transport from laser-target interactions. We have simulated the penetration of hot electrons through a cold electron background, where $\omega_p \Delta t \gg 1$ and $\Delta x/\lambda_D \gg 1$ both: (a) explicitly, by means of plasma period dilation [6], and, alternatively, (b) in the quasi-neutral limit, by using the implicit E field calculated from the electron momentum equation [7–9]. Together (a) and (b) have evolved into the Implicit Moment approach recently discussed elsewhere [10, 11] and detailed in the present paper. More recently, Denavit and Walsh [12] have reported the development of a similar approach to improve Denavit's time filtering technique.

* This work was performed under the auspices of the United States Department of Energy.

0021-9991/81/060233-12$02.00/0

2. The Advantages of Implicit E

Consider a one-dimensional, collisionless plasma consisting of ions and hot and cold electron components represented as particles. These are governed by the difference equations

$$u^{(m+1/2)} = u^{(m-1/2)} + \frac{q_\alpha E^{(*)}}{m_\alpha} \Delta t, \tag{1a}$$

$$x^{(m+1)} = x^{(m)} + u^{(m+1/2)} \Delta t, \tag{1b}$$

where (q_α, m_α) are $(-e, m)$ for electrons and (Ze, M) for ions, i.e., $\alpha \equiv h, c$ and i. In the conventional explicit leap-frog scheme $E^{(*)} = E^{(m)}$, and $E^{(m+1)}$ is computed at the beginning of the *next* cycle from Poisson's equation

$$\frac{\partial E^{(m+1)}}{\partial x} = 4\pi \sum q_\alpha n_\alpha^{(m+1)}, \tag{2a}$$

which differences as

$$\frac{E^{(m+1)}(i+\frac{1}{2}) - E^{(m+1)}(i-\frac{1}{2})}{\Delta x} = -4\pi e[n_e^{(m+1)} - Zn_i^{(m+1)}] \equiv -4\pi e \Delta n^{(m+1)}, \tag{2b}$$

in which i is the cell center index, and $n_e = n_c + n_h$ is the sum of the hot and cold electron densities.

Let $E(i-\frac{1}{2}) = 0$; then Eq. (2b) rearranges to

$$E(i+\tfrac{1}{2}) = -(\omega_p \Delta t)^2 \frac{\Delta x}{(\Delta t)^2} \frac{m}{e} \Delta n/n_e|_i \tag{3}$$

with $\omega_p^2 \equiv 4\pi e^2 n_e/m$. Suppose we set Δt so that an electron at the mean thermal hot speed $v_h > 0$ crosses a cell in a single time step, i.e., $\Delta x = v_h \Delta t$. Then the total energy change for such an electron in Δt is $\Delta \mathscr{E} = e\Delta\phi = -e\bar{E}\Delta x \equiv eE(i+\frac{1}{2})\Delta x/2$, or

$$\Delta \mathscr{E}/(\tfrac{1}{2}mv_h^2) = -(\omega_p \Delta t)^2 \Delta n/n_e. \tag{4}$$

With $\Delta n/n_e < 0.25$, $\omega_p \Delta t \leqslant 2$ can be tolerated. However, with $\Delta n/n_e = O(1)$, as at the coronal edge of a laser pellet, the use of large time steps, $\omega_p \Delta t \gg 1$, will expose the electrons to fields that are large enough to change the electron mean energy by many multiples in one time step, leading to extreme violation of energy conservation and rapid divergence of the calculations.

One can avoid these difficulties at large Δt by either artificially decreasing the plasma frequency, as under "plasma period dilation" [6], or by making all, or part, of the $E^{(*)}$ in Eq. (1a) implicit [7–11]. With $E^{(*)} \sim E^{(m+1)}$ the velocities can be controlled, so as to limit the particle excursions and, therefore, the accumulated density deviations $\Delta n^{(m+1)}$. Thus, $\Delta \mathscr{E}$ remains of order $mv_h^2 \equiv kT_h$.

3. The Scheme

The value of an implicit approach has been recognized for some time [13], but implementation has lagged, due to the assumed need for costly iteration of the particle trajectories. We skirt this problem, in first approximation: (1) by solving the lower fluid moment equations each cycle in conjunction with Poisson's equation for an implicit $E^{(*)}$, and then (2) by advancing the particle equation with this predicted electric field.

Equation (1a) is first replaced *on the average* by the particle momentum equations

$$j_\alpha^{(m+1/2)} = j_\alpha^{(m-1/2)} - \frac{1}{m_\alpha}\left[\frac{\partial \mathscr{P}_\alpha^{(+)}}{\partial x} - q_\alpha n_\alpha^{(m)} E^{(*)}\right] \Delta t. \tag{5a}$$

Here, $j_\alpha = n_\alpha U_\alpha$, and $\mathscr{P}_\alpha \equiv n_\alpha(kT_\alpha + m_\alpha U_\alpha^2)$ is the second moment sum over the particles, i.e., $m\sum u^2$. Equation (1b) is replaced by continuity

$$\tilde{n}_\alpha^{(m+1)} = n_\alpha^{(m)} - \frac{\partial}{\partial x} j_\alpha^{(m+1/2)} \Delta t. \tag{5b}$$

For one-dimensional problems we can integrate the Poisson equation, Eq. (2), obtaining

$$\tilde{E}^{(m+1)} = 4\pi \int_0^x \sum_\alpha q_\alpha \tilde{n}_\alpha^{(m+1)}\, dx + \tilde{E}^{(m+1)}(0), \tag{6}$$

where the integral is arbitrarily started at $x = 0$. The tilde on $\tilde{n}^{(m+1)}$ and $\tilde{j}^{(m+1/2)}$ in Eqs. (5) and (6) is notice that these quantities are predictions from the moment equations and not necessarily equal to the particle quantities $n^{(m+1)}$, $j^{(m+1/2)}$ that will be established in the next cycle. Thus, $\tilde{E}^{(m+1)}$ is the electric field consistent with these predictions.

The simplest and most stable choice for $E^{(*)}$ is the fully implicit field $E^{(*)} = E_i = \tilde{E}^{(m+1)}$. Alternatively, $E^{(*)} = E_c = \frac{1}{4}[E^{(m+1)} + 2E^{(m)} + E^{(m-1)}]$ is symmetric about (m), offering improved centering, and its levels are weighted, so as to smooth the electron accelerations. Thus, to introduce some flexibility, we have employed

$$E^{(*)} = \theta E_i + (1-\theta) E_c, \qquad 0 \leqslant \theta \leqslant 1. \tag{7}$$

Using this with Eqs. (5) and Eq. (6), we derive the predicted field

$$\tilde{E}^{(m+1)} = \frac{4\pi\left[\int_0^x \sum_\alpha q_\alpha n_\alpha^{(m)}\, dx - \sum_\alpha q_\alpha j_\alpha^{(m-1/2)} \Delta t + \sum_\alpha \frac{q_\alpha}{m_\alpha}\frac{\partial \mathscr{P}_\alpha^{(+)}}{\partial x}(\Delta t)^2\right] + B(x) + C(0)}{(1 + a\omega_p'^2 \Delta t^2)} \tag{8}$$

$\equiv [g(x) + C(0)]/f(x)$, in which $a \equiv \frac{1}{4}(3\theta + 1)$, $\omega_p'^2 \equiv 4\pi e^2(n_e + Z^2 n_i m/M)/m$, and $B(x) = \frac{1}{4}(1-\theta)[2E^{(m)} + E^{(m-1)}]$.

In Eq. (8), $C(0) = \tilde{E}^{(m+1)}(0) + 4\pi e \sum_\alpha \tilde{j}_\alpha^{(m+1/2)}(0)\,\Delta t$. At a specular or quiescent left boundary $j_\alpha(0) = E(0) = 0$, and, therefore, $C(0) = 0$. Alternatively, under periodic boundary conditions we require that $\phi(0) = \phi(L) - \int_0^L E\,dx$, and, thus, $C(0) = -\int_0^L gf^{-1}\,dx / \int_0^L f^{-1}\,dx$. From the particles we accumulate the fluid moments $n^{(m)}$, $j^{(m-1/2)}$, and $\mathscr{P}^{(+)}$ at the cell centers, but use the averaged values $j_{i+1/2}^{(m-1/2)} = [j^{(m-1/2)}(i) + j^{(m-1/2)}(i+1)]/2$ and $n_{i+1/2}^{(m)} = [n^{(m)}(i) + n^{(m)}(i+1)]/2$ in the calculations at cell boundaries for $\tilde{E}_{i+1/2}^{(m+1)}$. This implicit field is then area-weighted to the particle positions and used as $E^{(*)}$ each cycle in Eq. (1) to advance the particle coordinates.

Note that Nielson and Lewis [14] first used the fluid momentum equation in a particle code application to get a stable estimate for $\partial j/\partial t$, which is, of course, $[j^{(m+1/2)} - j^{(m-1/2)}]/\Delta t$. We have extended this notion to get $\tilde{j}_\alpha^{(m+1/2)}$ and $\tilde{n}_\alpha^{(m+1)}$ through the integrated difference expressions for the lower fluid moments, leading to our implicit solution of the Poisson equation for $\tilde{E}^{(m+1)}$.

For stability, when the time step is constrained to a Courant condition, $\Delta t \leqslant \Delta x/v_h$, and θ is chosen large enough, we have found it sufficient to accumulate $\mathscr{P}_\alpha^{(+)}$ from the mixed particle data at the end of a time step, i.e., from $[x^{(m)}, u^{(m-1/2)}]$. Stability at larger Δt and arbitrary θ has been achieved using the local adiabatic approximation, i.e., $\mathscr{P}_e^{(+)} = \mathscr{P}_e^{(m-1/2)}(n_e^*/n_e^{(m-1/2)})^3$, in which $n_e^{(*)} = Zn_i^{(m)} - (1/4\pi e)(\partial E^{(*)}/\partial x)$, and $n_e^{(m-1/2)}$ is accumulated at the half-time positions with $\mathscr{P}_e^{(m-1/2)} \equiv \mathscr{P}_h^{(m-1/2)} + \mathscr{P}_c^{(m-1/2)}$. In this approximation Eq. (8) is solved iteratively starting with the values of $E^{(*)}$ from the previous cycle.

In the quasi-neutral limit $\omega_p'^2 \Delta t \gg 1$ with $\theta = 1$ and for a specular boundary, $C(0) = 0$, when the $n_\alpha^{(m)}$ and $j_\alpha^{(m-1/2)}$ terms are neglected, Eq. (8) reduces to

$$\tilde{E}^{(m+1)} = 4\pi\omega_p'^{-2} \sum_\alpha \frac{q_\alpha}{m_\alpha} \frac{\partial \mathscr{P}_\alpha^{(+)}}{\partial x}, \tag{9}$$

which is equivalent to the result obtained by Hewett and Nielson [3, Eq. (38)], except that here $\mathscr{P}_\alpha^{(+)}$ is accumulated from the particles. When the ions are motionless ($M \to \infty$) this reduces to the familiar form

$$\tilde{E}^{(m+1)} = \frac{-\partial[\mathscr{P}_h^{(+)} + \mathscr{P}_c^{(+)}]}{en^{(m)}\partial x}. \tag{10}$$

If we remain in these limits with $C(0) = 0$, but now include the current terms $j^{(m-1/2)}$, Eq. (7) becomes

$$\tilde{E}^{(m+1)} = \frac{m[j_h^{(m-1/2)} + j_c^{(m-1/2)}]/\Delta t - \partial[\mathscr{P}_h^{(+)} + \mathscr{P}_c^{(+)}]/\partial x}{en_e^{(m)}}. \tag{11}$$

This is the collisionless limit of the "moment method" field first derived in Ref. [7]. It follows directly from setting $\tilde{j}_h^{(m+1/2)} + \tilde{j}_c^{(m+1/2)} = 0$, and solving Eq. (5a) for

$E^{(*)} = \tilde{E}^{(m+1)}$. If exact quasi-neutrality were achieved with this E every cycle, then $[j_h^{(m-1/2)} + j_c^{(m-1/2)}]$ would be zero, and Eq. (11) would go to Eq. (10). In fact, the predicted currents from Eq. (5a) at the end of each cycle will deviate, to some extent, from the actual currents that will be accumulated from the particle moments, and, thus, the $j_\alpha^{(m-1/2)}$ terms in Eq. (11) provide an E field component that acts to correct these deviations.

In Ref. [9] we indicated that, despite its tendency to eliminate error in the currents, the Eq. (11) E field allowed an accumulation of charge separation error in steep density gradient regions, such as pellet coronas. Plasma period dilation which yields less separation in such regions was, therefore, favored.

However, now, if we also retain the density term Eq. (11) becomes

$$\tilde{E}^{(m+1)} = \frac{-\int_0^x m\frac{[n_e^{(m)} - Zn_i^{(m)}]}{(\Delta t)^2}\,dx + m\frac{[j_h^{(m-1/2)} + j_c^{(m-1/2)}]}{\Delta t} - \frac{\partial}{\partial x}[\mathscr{P}_h^{(+)} + \mathscr{P}_c^{(+)}]}{en_e^{(m)}} \tag{12}$$

The new term acts to eliminate the charge separation errors. This is evident when we note that, by imposing quasi-neutrality on the predicted densities (instead of the currents), Eq. (5b), yields

$$\sum q_\alpha \tilde{n}_\alpha^{(m+1)} = 0 = \sum q_\alpha n_\alpha^{(m)} - \sum q_\alpha \frac{\partial}{\partial x}\tilde{j}_\alpha^{(m+1/2)}\Delta t, \tag{13a}$$

which integrates for the specular boundary to

$$\tilde{j}_h^{(m+1/2)} + \tilde{j}_c^{(m+1/2)} = \int_0^x [n_e^{(m)} - Zn_i^{(m)}]\,dx/\Delta t. \tag{13b}$$

This combines with Eq. (5a) to give the Eq. (12) $\tilde{E}^{(m+1)}$. The predicted currents from this field are, therefore, just those required to cancel previous density errors.

Thus, compared to the schemes in Refs. [6–9] for quasi-neutral plasmas, the present Implicit Moment approach is superior, by eliminating the charge separation errors, while avoiding the uncertainties associated with plasma period dilation.

More generality, the Eq. (8) field has a variety of desirable properties. In vacuum regions, $\omega_p^2 \to 0$, the field is determinant and finite, unlike the Eq. (10) result, and limits to the usual explicit Poisson values

$$\tilde{E}^{(m+1)} \to 4\pi \int_0^x \sum q_\alpha n_\alpha^{(m)}\,dx + \tilde{E}^{(m+1)}(0). \tag{14}$$

This is also true as $\Delta t \to 0$, with the $j_\alpha^{(m-1/2)}$ term providing a first order correction to the usual leap-frog field and, thus, a second order contribution to the particle speeds

$u^{(m+1/2)}$. The Eq. (8) field can be readily modified, so as to "soften" the effects of the correction terms, if desired, by the substitutions

$$4\pi \int_0^x \sum_\alpha q_\alpha n_\alpha^{(m)}\, dx \to \beta 4\pi \int_0^x \sum_\alpha q_\alpha n_\alpha^{(m)}\, dx + (1-\beta)[E^{(m)} - E^{(m)}(0)], \tag{15a}$$

$$4\pi \sum_\alpha q_\alpha j_\alpha^{(m-1/2)} \Delta t \to \gamma 4\pi \sum_\alpha q_\alpha j_\alpha^{(m-1/2)} \Delta t - (1-\gamma)[E^{(m)} - E^{(m-1)}] \tag{15b}$$

with the range $\beta, \gamma = 0 \to 1$ for the parameters. Thus far, however, we have found that $\beta = \gamma = 1$ give the most physical results. When $\beta = 0$, for example, the density correction is lost. This uncorrected limit is established directly, incidentally, should we start with Poisson's equation in its time derivative form, i.e., $\partial E/\partial t = -4\pi \sum q_\alpha j_\alpha^{(m+1/2)}$, instead of with Eq. (2a).

In simulations, we have found that the electrons gradually cool with the fully implicit, $\theta = 1$ field, so that the need for improved energy conservation has led us to consider the more general Eq. (7) $E^{(*)}$. Alternate generalizations are, of course, possible. For example, $E^{(*)} = \theta E^{(m+1)} + (1-\theta) E^{(m)}$ provides centering with $\theta = \frac{1}{2}$, when both the velocities and positions for the particles are stored at full times [levels $-(m)$]. However, this second formulation is more expensive computationally by requiring that $E^{(*)}$ be sampled at the extrapolated particle for time $(m+\theta)$. Similarly, the "time-filtered" centering, $E^{(*)} = \frac{1}{4}[3E^{(m+1)} + E^{(m-1)}]$, of Crystal *et al.* [4] and Denavit and Walsh [12] could be employed. This requires increased storage and extrapolations to sample $E^{(*)}$, but has the advantage that it applies damping preferentially to the highest frequency disturbances. On the other hand, this filtered centering always cools in the aggregate, and provides no option to "tune out" the damping in instances when energy conservation is required.

To investigate stability we have employed the linearized fluid equations for e^{ikx} disturbances of adiabatic electrons oscillating in a uniform motionless background, where the mean thermal speed is $a_0 = (kT/m)^{1/2}$, and the density is $n_0 = Zn_i$, i.e.,

$$\frac{\partial U_k}{\partial t} = -\frac{3a_0^2 ik}{n_0} \bar{n}_k + \frac{\omega_p^2}{ikn_0} \bar{\bar{n}}_k, \tag{16a}$$

$$\frac{\partial n_k}{\partial t} = -ikn_0 U_k, \tag{16b}$$

in which $E_k = -4\pi e n_k/ik$ has been eliminated. The use of Eqs. (16) is equivalent to assuming $\bar{n}_e = n_e$, $\bar{\bar{E}} = E$, etc. The densities $\bar{n}_k$ and $\bar{\bar{n}}_k$ are associated with the pressure and E field, respectively. Introducing the time dependencies $n_k = n_0 e^{i\omega(t-t_0)}$ and $U_k = U_0 e^{i\omega(t-t_0)}$ we get, for example, $n_k^{(m)} = n_0 e^{i\omega m \Delta t} = n_0 \xi^m$, with $\xi = e^{i\omega \Delta t}$, at the discrete levals $m = (t-t_0)/\Delta t$. Finally, by giving both $\bar{n}_K$ and $\bar{\bar{n}}_K$ time levels consistent with Eq. (7), i.e.,

$$\bar{n}_k = \bar{\bar{n}}_k = \left(\frac{1+3\theta}{4}\right) n_k^{(m+1)} + \left(\frac{1-\theta}{4}\right)[2n_k^{(m)} + n_k^{(m-1)}], \tag{17}$$

and using, for example, $\partial U_k/\partial t = [U_k^{(m+1/2)} - U_k^{(m-1/2)}]/\Delta t$, we derive the dispersion relation

$$(\xi - 1)^2 = -(c^2/4)[(1 + 3\theta)\,\xi^2 + 2(1 - \theta)\,\xi + (1 - \theta)], \tag{18}$$

where

$$c^2 = (\omega_p^2 + 3a_0^2 k^2)\,\Delta t^2 \equiv \bar{\omega}_p^2 \Delta t^2.$$

In the fully implicit, $\theta = 1$ limit Eq. (18) has the solution $\xi = (1 \pm ic)^{-1}$, so the amplification factor is $|\xi| = (1 + c^2)^{-1/2}$. Let $\xi \equiv e^{i\omega\Delta t} = e^{i\omega_0\Delta t}e^{-\gamma\Delta t}$. Then, $|\xi| = e^{-\gamma\Delta t} = 1/c = 1/\bar{\omega}_p\Delta t$ for $c \gg 1$, and $\gamma = 1/\Delta t\,\log(\bar{\omega}_p\Delta t)$. The scheme is stable, but disturbances decay away in a time $T_d = 1/\gamma = \Delta t/\log(\bar{\omega}_p\Delta t)$. Alternatively, in the fully centered limit, $\theta = 0$, $\xi = (1 \pm ic/2)/(1 \mp ic/2)$, so $|\xi| = 1$ and for arbitrary c there is neither damping or growth. Further, when $c \gg 1$, $\xi = -1$ so $e^{i\omega\Delta t} = \cos\omega_0\Delta t = -1$, and $\omega_0\Delta t = 2\pi\Delta t/T = \pi$ yield oscillations for the disturbances at period $T = 2\Delta t$. Next, for arbitrary θ and $c \gg 1$, Eq. (18) yields $|\xi| = |(1 - \theta)/(1 + 3\theta)|^{1/2}$, which is always $\leqslant 1$. Thus, with a small non-zero θ it should be possible to remove the $2\Delta t$ oscillations, if this is desired. Finally, we note that for $c \gg 1$ and any θ, $\xi \to 1 \pm ic$, so $e^{i\omega\Delta t} \to 1 + i\omega\Delta t$ yields $\omega \to \pm(\omega_p + 3a_0^2k^2)^{1/2}$ and plasma oscillations are returned.

To explore the $\theta = 0$ case further consider the family of centered choices

$$\bar{n}_k = \bar{\bar{n}}_k = \delta n^{(m+1)} + (1 - 2\delta)\,n^{(m)} + \delta n^{(m-1)}, \qquad \delta \geqslant 0. \tag{19}$$

Used with Eqs. (16) this yields the standard explicit leap-frog scheme for $\delta = 0$, and our implicit centered scheme for $\delta = \frac{1}{4}$. From the dispersion relation obtained with this family, we find that the amplification factor $|\xi|$ is unity for $c^2 \leqslant 4/(1 - 4\delta)$; for larger c, $|\xi|$ exceeds unity, indicating unstable growth. This verifies that the explicit leap-frog scheme is unstable for $\omega_p\Delta t > 2$, as asserted with Eq. (4), while the $\theta = 0$ scheme of Eqs. (7) and (17), is stable for any value of $\omega_p\Delta t$. For $\delta \geqslant \frac{1}{4}$ we find that with $c \gg 1$ the maximum frequency permitted disturbances is $\omega_0 = 2/\Delta t$ $\sin^{-1}|1/(2\sqrt{\delta})|$. At $\delta = \frac{1}{4}$ these are oscillations of period $T = 2\Delta t$. With larger δ they would be at progressively lower frequency, implying an unnecessary distortion of the dispersion relation. Thus, with $\delta = \frac{1}{4}$ we smooth our results by imposing a ceiling on the disturbances at the maximum frequency resolvable and consistent with stability. Any damping from $\theta \to 0$ provides additional smoothing. Thus, despite the statistical errors associated with the accumulation of the current and pressure fluid moments, in simulation we have found that the implicit method gives smoother results than those obtained via corresponding explicit leap-frog calculations. It is possible that even smoother results at greater computational efficiencies will derive from the use of "orbit averaging" [5] in conjunction with the implicit moment method.

An important consideration is the maximum time step permitted with the implicit method. To examine this we use Eq. (17) for $\bar{\bar{n}}_k$ but set

$$\bar{n}_k = \varepsilon\bar{\bar{n}}_k + (1 - \varepsilon)\,n_k^{(m)}, \qquad 0 \leqslant \varepsilon \leqslant 1, \tag{20}$$

corresponding to a fully explicit $\mathscr{P}_\alpha^{(\dagger)}$ when $\varepsilon = 0$. Then, for a fully implicit field, but an explicit pressure ($\theta = 1, \varepsilon = 0$), when $c \gg 1$, the largest root of the dispersion relation is $\xi = ka_0/\omega_p \simeq \lambda_D/\Delta x$. Since for applications of interest $\Delta x \gg \lambda_D$, $|\xi|$ is always less than unity. Thus, theoretically any Δt should be permitted. This limit is an exception, however, and is, in fact, not observed in simulation. For smaller θ, Δt must be bounded for stability, and when $\theta = 0$, there should be unstable growth unless $a_0 = 0$. These results are unchanged if $\bar{n}_k = n_k^{(m-1)}$, and should, therefore, apply for our mixed-level $\mathscr{P}_\alpha^{(\dagger)}$. Indeed, in simulation we observe a gradual heating when $\theta = 0$. In practice, with explicit $\mathscr{P}_\alpha^{(\dagger)}$ the heating has been eliminated, by keeping $\Delta t < \Delta x/v_h$, and tuning θ to an appropriate value. Thus, for the sample applications which follow, pressure was explicit and $\theta = 0.38$ was found to be optimal so that, for example, in the two-stream, $\omega_p \Delta t = 0.4$, problem, which we will describe, energy was conserved to within 1% over 3000 cycles.

Brackbill (see [15]) first alerted us to the time step limitation imposed by the pressure gradient terms in Eq. (5a), suggesting that the use of $\mathscr{P}_\alpha^{(\dagger)} = a_0 = 0$ would allow arbitrary Δt. Our computational experience confirms this for $\theta = 1$. We find, however, that our local adiabatic approximation for the pressures gives equal stability with superior energy conservation and precision, e.g., two-stream eddies, damped at large Δt when $\mathscr{P}_\alpha^{(\dagger)}$ is set to zero, remain preserved under the local adiabatic approximation. Of course, for accuracy Δt must still be small enough so that field structures of interest are sampled several times during the transit of a typical particle. Presumably, the local adiabatic approximation can be generalized, by getting $\mathscr{P}_e^{(\dagger)} = \mathscr{P}_e^{(*)}$ not from $\mathscr{P}_e^{(\dagger)} \sim n_e^3$ but from the implicit solution to the next higher, energy moment equation under the assumption of a zero third moment, $q_\alpha = \Sigma (u - U_\alpha)^3 = 0$. Alternatively, here, one might choose to use $q_\alpha^{(\dagger)} = q_\alpha^{(m-1/2)}$.

Finally, we recall that ideally, the tilde densities and currents predicted with Eq. (5) should agree with the particle properties accumulated in the next step, i.e., $\tilde{j}^{(m+1/2)} \to j^{(m+1/2)}$, $\tilde{n}^{(m+1)} \to n^{(m+1)}$. Then in the quasi-neutral limit, for example, the correction terms e.g., $\sum q_\alpha j_\alpha^{(m-1/2)}$, are actually zero, and improved energy conservation can be anticipated. Improvements correcting for the differences between the fluid and finite particle descriptions are, therefore, desirable. These may include iterating on E and the particle equations, using the Eq. (8) field as a first guess.

4. Sample Applications

A. *One- and Two-Temperature Expansions*

As an example, we have looked at the one-dimensional expansion of collisionless plasma into a vacuum. The simulations package is more generally used to study laser–plasma interactions, so the input and output are dimensional with time in picoseconds and distance in microns. Wet set $Zn_i = n_e = 5 \times 10^{21}\ \mathrm{cm}^{-3}$ initially, and $n_c = 0$ with $T_h = 10\ \mathrm{keV}$ and $T_i = 1\ \mathrm{keV}$. We used 100 cells at $\Delta x = 0.5\ \mu\mathrm{m}$ and $\Delta t = 10^{-3}$ psec. Here $v_h = 42.4\ \mu\mathrm{m/psec}$ so that the Courant condition on the

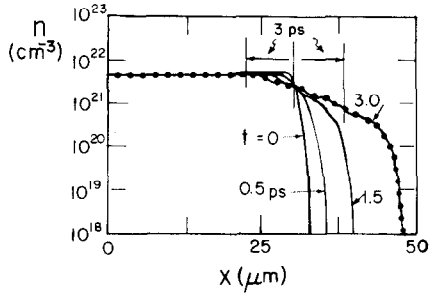

FIG. 1. n_e and Zn_i curves for the expansion of a $Z = 10$, $A = 25$ plasma with $T_e/T_i = 10$. Evolution to $\omega_p \Delta t = 1.2 \times 10^4$ with $\omega_p \Delta t = 4$, $\Delta x/\lambda_D = 47.8$.

electrons actually permits a time step at least five times larger. This has been subsequently tried and gives nearly identical results.

This calculation ran 3000 cycles with $Z = 10$, $A = M/M_p = 100$, where M_p is the mass of a proton, here reduced to speed the calculations. We employed only 2×10^3 particle-electrons and an equal number of ion particles. Before submission as sources into the Eq. (7) field expression, the density, current and pressure moments were smoothed by passing them through the operator $O(A) \equiv \frac{1}{4}[A(i+1) + 2A(i) + A(i-1)]$. This was done four times each cycle. The results are essentially unaltered (but noisier), when this smoothing is omitted. In the dense, unexpanded plasma $\omega_p = 4\pi \times 10^3$ psec^{-1}, so $\Delta x/\lambda_D = 47.8$ and $\omega_p \Delta t = 4.0$. The ion acoustic speed $v_{i.a.} = (ZT_e/M)^{1/2} = 2.7\,\mu$m/psec. The boundaries are specular.

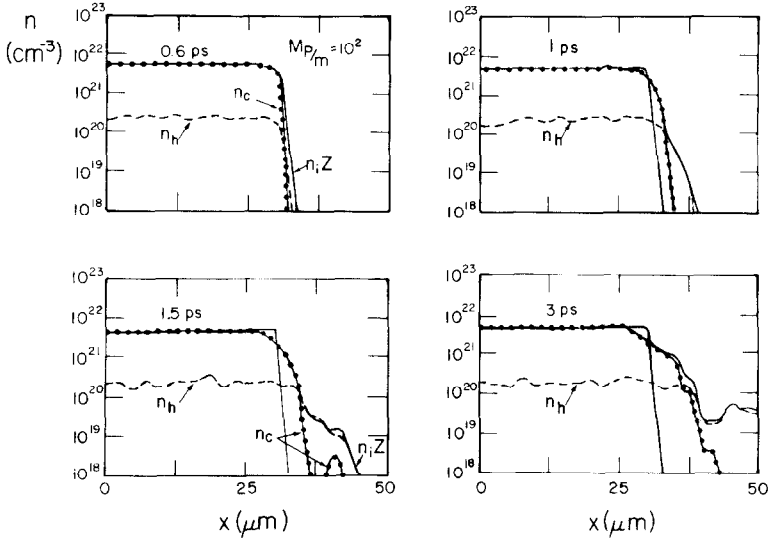

FIG. 2. Two-temperature electron driven expansion: $T_h/T_c = 3.3$, and $T_h/T_i = 10.0$.

Figure 1 gives the results of the calculation. The vertical fiducial lines mark the distance traveled in 3 psec by a particle moving at the ion-acoustic speed. Each curve is actually two overlaid curves—one for n_e and one for Zn_i—but the Eq. (7) field, here in its quasi-neutral limit, locks them into superposition. Incidently, T_h remains nearly isothermal over the run.

For the Fig. 2 sequence, we have reduced the hot density to 5% of the total, $n_h = 2.5 \times 10^{20}\,\mathrm{cm}^{-3}$. We set the main body of cold electrons at $T_c = 3\,\mathrm{keV}$ and $T_i = 3\,\mathrm{keV}$. We used 10^3 cold electron particles and 10^3 hot particles; so the resolution of the electron distribution "tail" was increased, at least, 10-fold. Otherwise, the parameters were unchanged. Upon expansion the hot electrons rapidly fill the low density "coronal" region, which is followed by the slower expansion of the plasma main-body. Eventually, the fastest ions are reflected off the right computational boundary at $x = 50\,\mu\mathrm{m}$.

B. *Two-Beam Instability*

For a second test we have applied the implicit method to the two-beam problem in a warm plasma. The beam drift speeds v_d were $\pm 25\,\mu\mathrm{m/psec}$, respectively, and the beam temperatures were 0.43 keV, so that their mean thermal speeds $v_h = (T/m)^{1/2} = 8.8\,\mu\mathrm{m/psec}$ and, thus, $v_p \equiv \sqrt{2}\,v_h = 12.5\,\mu\mathrm{m/psec}$, giving $|v_d| = 2v_p$. We used 10^4 simulation particles in each beam, 100 cells, and, of course, periodic boundary conditions. The total density, i.e., from both beams, was $n_e = 10^{21}\,\mathrm{cm}^{-3}$, so that $\omega_p^{-1} = 5.61 \times 10^{-4}\,\mathrm{psec}$ and $\lambda_D = v_h/\omega_p = 4.87 \times 10^{-7}\,\mathrm{cm}$. The ions were stationary ($M \to \infty$).

In our first calibrational run $\Delta t = 2.24 \times 10^{-4}\,\mathrm{psec} = 0.4\,\omega_p^{-1}$ and $\Delta x = 2.43 \times 10^{-6}\,\mathrm{cm} = 5.0\,\lambda_D$. This was, therefore, equivalent to Case V, in Ref. [16] by Morse and Nielson, except that our time step was 2.5 times larger, and our cell size was five times larger. Frame (a) of Fig. 3 shows the starting conditions. The particles were

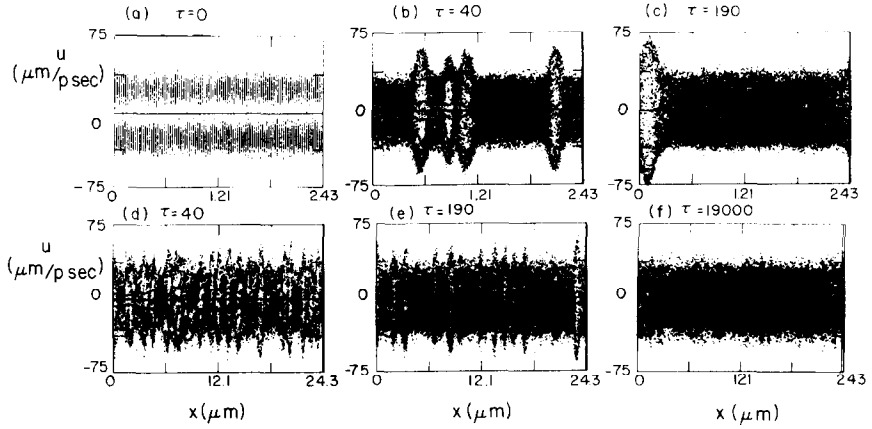

FIG. 3. Two-beam instability in a warm plasma calculated with: (a)–(c) $\omega_p \Delta t = 0.4$, (d)–(e) $\omega_p \Delta t = 4.0$, and (f) $\omega_p \Delta t = 40.0$.

loaded at cell centers. Frame (b) shows the development at 40 plasma periods, i.e., $\tau = t/T = \omega_p t/2\pi = 40$, $\omega_p t = 251$, after 620 cycles. The coalescing eddies of Ref. [16] are very much in evidence. We see four or five eddies over the 500 λ_D test area, as did Morse and Nielson for comparable times. Of course, slightly different initial conditions, and our large Δt and Δx, should alter the details. Frame (c) shows the results when we let the calculation continue to $\tau = 190$, cycle 3000. Smearing and coalescence of the eddies have reduced their number to 1.

Figure 3 frames (d) and (e) show the results of running the calculation with $\omega_p \Delta t = 4.0$, and $\Delta x/\lambda_D = 50.0$. After 62 cycles we get frame (d), $\tau = 40$, which shows approximately three or four eddies in the right 10 % of the test area, in agreement with frame (b). The two horizontal curves through the beams are the mean currents, e.g., $j_h = n_h v_h$. By $\tau = 400$ (100 cycles) we obtain frame (e), which is comparable to (c). It exhibits about 12 eddies over the full 5000 λ_D test area. As a general rule, we have found that instability sets in later, as we increase $\omega_p \Delta t$, but that comparable turbulent states, as limited by the reduced resolution at larger Δx, are achieved at large times. Frame (f), for example, is the result obtained after 3000 cycles with $\omega_p \Delta t = 40$ and $\Delta x/\lambda_D = 500$ at time $\tau = 19{,}000$. The left 10 % of frame (f) is equivant to the frame (e) result run 100 times longer. This would, incidentally, correspond to a 67-psec interval and a 243-μm test area, consistent with the corona of a laser pellet.

These two-stream results must be viewed with caution. For cold beams the maximum growth should occur near $k = \omega_p/|v_d| = 7.1 \times 10^5\ \mathrm{cm}^{-1}$, at a rate near $|\gamma| = \omega_p/2$. Assuming the smallest rate resolvable is $\lambda_{min} = 2\Delta x$, we get $k_{max} = 12.9 \times 10^5$, 1.79×10^5, and $0.129 \times 10^5\ \mathrm{cm}^{-1}$ for the three cases considered. So only in the first case is $|\gamma|\Delta t < 1$, and only in this case is the fastest growing mode resolved. In the remaining cases the scheme will attribute the beam coupling to more slowly growing modes. Similarly, non-linear trapping of the electrons is characterized by a rate $\omega_t = (e\phi/kT)^{1/2} k \lambda_D \omega_p$. At $\tau = 40$ when four eddies are visible in Fig. 3b we find that $e\phi = 8$ keV at the eddy peaks, while the background has heated to $kT = 2$ keV. The length of the eddies is roughly $L = 8\Delta x = 40\lambda_D$ ($T = 0.43$ keV) $= 18.6\ \lambda_D$ ($T = 2$ keV), so $k = 2\pi/L = 0.34/\lambda_D$. Thus, $\omega_t = (8/2)^{1/2}\, 0.34\ \omega_p = 0.68\ \omega_p$. For our three cases $\omega_p \Delta t = 0.4$, 4.0, and 40.0, therefore, we see $\omega_t \Delta t = 0.27$, and 27.0. Only our first case has a reliable $\Delta t < \omega_t^{-1}$, although $\Delta t < T_t = 2\pi\omega_t^{-1}$ may be sufficient, since our $\omega_p \Delta t = 4.0$ run crudely reproduces the $\omega_p \Delta t = 0.4$ structure. The crucial point here is that even our calculations for $|\gamma|\Delta t \gg 1$, $k_{max}\Delta x \gg 1$ and $\omega_t \Delta t \gg 1$ are stable and physically plausible. If greater detail in the evolving structure is desired, smaller time and space steps are still required.

5. Concluding Comments

We have demonstrated that the Implicit Moment approach can give stable, physically acceptable results for plasma simulations in which $\omega_p \Delta t > 2$ may be required for economy. The use of $(\omega_p \Delta t)(\Delta x/\lambda_D) = (4)(47.8) = 191.2$ for our Fig. 1

study implies, for example, an $O(200)$-fold speedup over conventional methods. The limits of accuracy of the implicit simulations need, however, to be explored, and the optimal tuning (through α and β, for example) and centering (as with Eq. (7)) must be defined. Even greater efficiencies may be envisioned with each particle advanced according to its own time step, and the fields calculated on the time scale over which they change appreciably. Additions including classical collisional effects, as initiated in Refs. [6–9], are needed for cold, high density laser pellet applications, and extension of the implicit approach to two dimensions, including B fields, offers, we think, a manageable and attractive challenge.

ACKNOWLEDGMENTS

The author is grateful to D. Forslund, C. Cranfill, J. Brackbill, W. Gula, and E. Lindman at Los Alamos for many helpful discussions and much encouragement.

REFERENCES

1. R. J. MASON, *Phys. Fluids* **14** (1971), 1943.
2. D. W. FORSLUND, J. M. KINDEL, K. E. LEE, AND E. L. LINDMAN, *Phys. Rev. Lett.* **36** (1976), 35.
3. D. W. HEWETT AND C. NIELSON, *J. Comput. Phys.* **24** (1978), 219.
4. T. L. CRYSTAL, J. DENAVIT, AND C. E. RATHMANN, *Comments Plasma Phys.* **5** (1979), 17–28.
5. B. I. COHEN, T. A. BRENGLE, D. B. CONLEY, AND R. P. FREIS, Lawrence Livermore Laboratory Report UCRL-82832 (1979).
6. R. J. MASON, *Phys. Rev. Lett.* **43** (1979), 1795.
7. R. J. MASON, *in* "Proceedings, 11th European Conference on Laser Interactions with Matter, Sept. 19–23, 1977"; *Bull. Amer. Phys. Soc.* **22** (1977), 1188; *Bull. Amer. Phys. Soc.* **23** (1978), 856; *in* "Proceedings, 9th Anomalous Absorption Conference, Rochester, N.Y., May 1979", paper B-9, and *in* "Proceedings, Fifth Laser Workshop on Laser Interactions with Matter, Rochester, N.Y., Nov. 5–9, 1979", Plenum, in press.
8. R. J. MASON, *in* "Proceedings, Informal Conference on Particle and Hybrid Codes for Fusion, Napa, Calif., Dec. 10–11, 1979," University of California, Berkeley, Electronics Research Laboratory Memorandum No. UCB/ERL M79/79, paper 23.
9. R. J. MASON, *Phys. Fluids* **23** (1980), 2204.
10. R. J. MASON, *in* "Proceedings, 1980 IEEE International Conference on Plasma Science, Madison, Wisc., May 19–21, 1980," paper IB1.
11. R. J. MASON, *in* "Proceedings, 10th Annual Anomalous Absorption Conference, S. San Francisco, Calif., May 27–30, 1980," paper A10.
12. J. DENAVIT AND J. M. WALSH, *in* "Proceedings, Ninth Conference on Numerical Simulation of Plasmas, Northwestern University, June 30–July 2, 1980," paper PC-3.
13. A. B. LANGDON, *J. Comput. Phys.* **30** (1979), 202.
14. C. W. NIELSON AND H. R. LEWIS, "Methods in Computational Physics" (B. Alder, S. Fernbach, and M. Rotenberg, Eds.), Vol. 16, pp. 367, Academic Press, New York, 1976.
15. J. U. BRACKBILL AND D. W. FORSLUND, *Bull. Amer. Phys. Soc.* **25** (1980), 973; and to be published.
16. R. L. MORSE AND C. W. NIELSON, *Phys. Fluids* **12** (1969), 2418.